

1 **Evaluation of a fully human, hepatitis B virus-specific chimeric antigen**
2 **receptor in an immunocompetent mouse model**

3
4 Marvin M. Festag¹, Julia Festag¹, Simon P. Fräßle², Theresa Asen¹, Julia Sacherl¹,
5 Sophia Schreiber¹, Martin Mück-Häusl¹, Dirk H. Busch^{2,3}, Karin Wisskirchen^{1,3*} and
6 Ulrike Protzer^{1,3*}.

7 *both authors contributed equally to the work

8
9 1 Institute of Virology, Technische Universität München / Helmholtz Zentrum
10 München, 81675 Munich, Germany.

11 2 Institute for Medical Microbiology, Immunology and Hygiene, Technical University
12 of Munich, 81675 Munich, Germany.

13 3 German Center for Infection Research (DZIF), Munich partner site, 81675 Munich,
14 Germany.

15
16 **Corresponding Author:** Prof. Ulrike Protzer, MD

17 Institute of Virology
18 Trogerstrasse 30, 81675 Munich, Germany
19 Phone: +49-89-4140-6821, Fax: +49-89-4140-6823
20 E-mail: protzer@tum.de; protzer@helmholtz-muenchen.de

21
22 Karin Wisskirchen, PhD
23 Institute of Virology
24 Trogerstrasse 30, 81675 Munich, Germany
25 Phone: +49-89-4140-6814, Fax: +49-89-4140-6823
26 E-mail: karin.wisskirchen@helmholtz-muenchen.de

27
28 **Short title:** Evaluating a human CAR in immunocompetent mice
29

30 **ABSTRACT**

31 Chimeric-antigen-receptor (CAR) T-cell therapy is a promising novel therapeutic
32 approach for cancer but also for chronic infection. We have developed a fully human,
33 second generation CAR directed against the envelope protein of hepatitis B virus on
34 the surface of infected cells (S-CAR). The S-CAR contains a human B cell-derived
35 single-chain antibody fragment and human IgG-spacer, CD28 and CD3 signaling
36 domains that may be immunogenic in mice. Because immunosuppression will
37 worsen the clinical course of chronic hepatitis B, we aimed at developing a preclinical
38 mouse model that is immunocompetent and mimics chronic hepatitis B but
39 nevertheless allows evaluating efficacy and safety of a fully human CAR. The S-CAR
40 grafted on T cells triggered antibody responses in immunocompetent animals, and a
41 co-expressed human-derived safeguard EGFRt even induced B- and T-cell
42 responses - both limiting the survival of S-CAR-grafted T cells. Total body irradiation
43 and transfer of T cells expressing an analogous, signaling-deficient S-CAR-decoy
44 and the safeguard induced immune tolerance towards the human-derived structures.
45 S-CAR T cells transferred after immune recovery persisted and showed long-lasting
46 antiviral effector function. The approach we describe herein will enable preclinical
47 studies of efficacy and safety of fully human CARs in the context of a functional
48 immune system.

49

50 **INTRODUCTION**

51 T-cell therapies utilizing chimeric antigen receptors (CARs) have emerged as a
52 revolutionary approach to treat cancers and infections with a high specificity during
53 the last two decades.¹ Anti-CD19 CAR T-cell therapy has a significant benefit for
54 patients with B-cell malignancies not responding to first-line chemo- and immune
55 therapies and recently two CAR T-cell products have been approved for clinical use.²
56 ³ CAR T cells for other cancer types including solid tumors have also been developed
57 and are currently evaluated in clinical trials. However, it became obvious that CAR T-
58 cell therapy of solid tumors is a more complex scenario.⁴ Targets for CAR T-cell
59 therapies include tumor-associated antigens but also viral antigens displayed on the
60 surface of malignant or infected cells. CARs that exploit binders recognizing viral
61 envelope proteins have been developed for chronic infections with hepatitis B virus
62 (HBV),⁵ human cytomegalovirus,⁶ hepatitis C virus,⁷ and human immunodeficiency
63 virus.^{8,9}

64 A CAR is composed of a single-chain variable fragment (scFv) that determines the
65 target specificity, an extracellular spacer linking the scFv to the signaling domains, a
66 transmembrane domain and intracellular signaling domains. In clinical application,
67 ideally a fully human CAR should be utilized to prevent rejection of CAR T cells by
68 the patient's immune system. Furthermore, accessory molecules co-expressed to
69 purify CAR T cells or as a safeguard to be able to deplete T cells if needed could also
70 be recognized as foreign if they contain non-human-derived domains. In fact, CAR T
71 cells carrying a murine scFv were rejected and their use lead to decreased response
72 rates in patients.¹⁰

73 Before advancing to clinical application, CAR constructs have to be studied in
74 preclinical models. In particular, immunocompetent preclinical models are urgently
75 needed to study the efficacy but also potential side effects of a CAR T-cell therapy,
76 because these can be largely influenced by bystander effects of other immune cells
77 or mediators. Immune competence of the animals, however, can limit the preclinical
78 investigation of a CAR with human domains since allogenic immune rejection could
79 limit CAR T-cell persistence in these models. To prevent such an immune response
80 by the endogenous murine immune system, most preclinical studies are performed in
81 immunodeficient mouse models.¹¹ In the case of anti-CD19 CAR T-cell transfer for
82 hematological malignancies, patients are preconditioned with chemotherapeutic
83 lymphodepleting regimens and hence, using immunodeficient mice mimics this
84 particular clinical situation.¹² However, immunosuppressive or lymphodepleting
85 regimens will most likely not be applied in the clinics for CAR T-cell approaches
86 targeting certain solid tumors or fighting viral diseases. We therefore aimed at
87 generating an experimental, preclinical system in which the recipient is
88 immunocompetent and which at the same time allows the study of CARs with
89 human-derived sequences.

90 The target of the CAR T-cell approach presented here is HBV. Chronic hepatitis B
91 and HBV-associated hepatocellular carcinoma (HCC) are a major health concern
92 with >250 million humans affected and 880,000 deaths per year due to HBV-
93 associated liver diseases.¹³ Current treatment regimens suppress viral replication but
94 are curative only in rare cases. HBV still is the major cause of HCC development
95 worldwide and mainly due to a lack of therapeutic options, HCC became the number
96 two cause of cancer-related death.¹⁴ CAR T-cell therapy is a promising approach to
97 address this medical need¹⁵.

98 We have generated a fully human CAR that is specific for the small envelope protein
99 “S” of HBV and targets the S-domain (S-CAR) of all HBV envelope proteins,⁵ which
100 are found on the surface of HBV virions and subviral particles therefore called
101 hepatitis B surface antigen (HBsAg), but are also located on the surface of HBV-
102 infected hepatocytes and HBV-induced hepatoma cells.¹⁶ Previous results from our
103 laboratory indicated that the S-CAR can redirect T cells against HBV-infected
104 hepatocytes *in vitro* and eliminate HBV from infected cell cultures⁵ but that the
105 therapeutic effect of adoptively transferred murine S-CAR T cells into HBV-transgenic
106 immunocompetent mice was limited.¹⁷ After an initial expansion and a very good
107 antiviral effect, S-CAR T cells vanished and viral parameters rose again.

108 In the study presented here, we show that an immune response against the human
109 domains of the S-CAR limited CAR T-cell persistence in immunocompetent
110 preclinical mouse models but not in immunocompromised animals. We were able to
111 overcome the problem of S-CAR T-cell rejection by specifically tolerizing
112 immunocompetent mice against the allogenic CAR domains. In this setting, S-CAR T
113 cells persisted at high numbers and induced a sustained antiviral effect.

114

115 **RESULTS**

116 **A repeated transfer of S-CAR T cells into immunocompetent mice does not** 117 **lead to quantitative or functional reconstitution of S-CAR T cells**

118 A loss of S-CAR T-cell function that has been observed after transfer into HBV-
119 transgenic mice¹⁷ could be due to either T-cell exhaustion or activation-induced cell
120 death or an immune response against the transferred cells. To address this question,

121 we investigated whether a second transfer of S-CAR T cells would maintain the
122 antiviral effect. We engineered murine CD45.1⁺ CD8⁺ T cells to express the S-CAR
123 (schematically depicted in Figure S1) and transferred them on day 0 and again on
124 day 20 into CD45.1-negative HBV-transgenic mice. A second group of mice received
125 the T-cell product only on day 20 (Figure 1A). The congenic marker CD45.1 allowed
126 to differentiate transferred cells from endogenous, CD45.2⁺ cells. We detected
127 comparable numbers of total CD45.1⁺ transferred cells on day 25, i.e. five days after
128 first or second transfer that dropped until day 33, i.e. two weeks after transfer, in both
129 groups (Figure 1B). In contrast to total transferred cells, S-CAR-expressing T cells
130 were only detected after the first but not after the second transfer (Figure 1C).
131 Concomitantly, liver damage indicated by a rise in serum alanine amino transferase
132 (ALT) levels five to seven days after transfer was exclusively detected after the first
133 but not after the second injection of S-CAR T cells (Figure 1D). On day 33,
134 lymphocytes from liver and spleen were isolated and stimulated on plate-bound
135 HBsAg, or anti-CD3/anti-CD28 antibodies as positive control. Phosphate-buffered
136 saline (PBS)-treated plates served as negative control. Intracellular cytokine staining
137 (ICS) did not reveal HBsAg-specific activation of lymphocytes (Figures 1E and S2),
138 although a comparable S-CAR signal was still detected by qPCR in both groups
139 (Figure S3). The fact that neither S-CAR T cells nor liver cytotoxicity were detected
140 after the second adoptive transfer suggested an immune response against the
141 transferred cells rather than a lack of antigenic stimulation or T-cell exhaustion – both
142 of which would not lead to reduced cell numbers in a short term - or activation-
143 induced cell death.

144

145 **Adaptive immunity limits S-CAR T-cell persistence**

146 To find out if the murine immune system would react to the human-derived domains
147 on S-CAR T cells, we first transferred T cells that expressed the S-CAR or a non-
148 functional S-decoy (Δ)-CAR, both in combination with a truncated human epidermal
149 growth factor receptor (EGFRt), into HBV-naïve C57BL/6J mice. The S Δ -CAR
150 construct¹⁷ contains the same extracellular domains as the S-CAR, but intracellular
151 T-cell signaling domains have been exchanged to the cytoplasmic domain of the
152 nerve growth factor receptor rendering the S Δ -CAR incapable of activating T cells
153 (Figure S1). EGFRt can be targeted by depleting antibodies and serves as a potential
154 safeguard when *in vivo* toxicity is observed, but also as an additional transduction
155 and selection marker.^{18, 19} Both CARs contain a mutated, human IgG1 spacer with
156 decreased Fc-receptor binding capacity (Figure S1).²⁰ The T-cell products had
157 transduction rates of 85 % (S-CAR⁺/EGFRt⁺) or 74 % (S Δ -CAR⁺/EGFRt⁺) as
158 determined by flow cytometry (Figure 2A). Expansion and persistence of S-CAR and
159 S Δ -CAR T cells were limited in immunocompetent animals compared to that of mock
160 T cells without transgene expression, although all cell products were detected at
161 comparable numbers on day 3 (Figure 2B). When we transferred S-CAR or S Δ -CAR
162 T cells into B- and T-cell deficient Rag2^{-/-} mice, cells expanded and persisted at least
163 as well as mock T cells (Figure 2B). Hence, S-CAR and S Δ -CAR T cells vanished
164 irrespectively of presence of antigen or ability of CAR T cells to be activated, but only
165 in immunocompetent mice and not in immunodeficient mice. This indicated that
166 neither a lack of antigenic stimulation nor tonic signaling is the leading cause of S-
167 CAR T-cell depletion but that an immune response caused the fate of S-CAR T cells.

168 To investigate the antiviral potential of S-CAR T cells in the absence of anti-CAR
169 immunity, we adoptively transferred the cells into AAV-HBV-infected Rag2^{-/-}/IL-2Rγ^{-/-}
170 mice. AAV-mediated HBV genome transfer to the mouse liver allows persistence of
171 the HBV genome over months²¹ generating a preclinical model that *a priori* allows to
172 study not only HBV persistence but also “HBV cure”. A cure can be achieved in AAV-
173 HBV-infected mice because only a proportion of hepatocytes is infected and the HBV
174 genome remains episomal allowing elimination of infected hepatocytes. In AAV-HBV-
175 infected Rag2^{-/-}/IL-2Rγ^{-/-} mice, S-CAR T cells expanded and were detected for >30
176 days after transfer (Figure 2C). S-CAR T-cell therapy induced moderate liver damage
177 indicated by a transient increase of serum transaminase activity (ALT) to 70-190 U/l
178 (Figure 2D). To assess the antiviral activity of S-CAR T cells, we determined viral
179 HBsAg (Figure 2E) and e antigen (HBeAg) (Figure 2F) in serum. Notably, HBsAg
180 significantly decreased by about 2 log₁₀ until day 13 and then remained detectable at
181 a low level. HBeAg decreased more slowly by 60 % until day 38. These results
182 indicated that S-CAR T cells expand and exhibit a continuous antiviral effect if they
183 are not targeted by an adaptive immune response.

184

185 **Immunocompetent mice mount CD8⁺ T-cell and antibody responses against S-** 186 **CAR T cells**

187 As shown in Figure 2B, S-CAR T cells persisted in Rag2^{-/-} mice that harbor functional
188 NK cells, but neither B nor T cells. Hence, both B and T cells could be responsible for
189 reduced survival of S-CAR T cells. When we analyzed expression of either S-CAR or
190 EGFRt by flow cytometry after T-cell transfer, both markers disappeared in
191 immunocompetent but not in immunodeficient mice (Figures 3A and S4), confirming

192 the loss of S-CAR T cells. Next, we determined if T-cell responses contributed to S-
193 CAR T-cell rejection in the immunocompetent animals. Thus, we co-cultured
194 splenocytes from wildtype recipient mice that had received 2.7×10^6 T cells grafted
195 with both the S-CAR and the EGFRt overnight with CD8⁺ T cells as target cells
196 expressing either the S-CAR or the EGFRt. ICS revealed that endogenous CD45.2⁺
197 CD8⁺ T cells from the treated mice became activated and expressed IFN- γ if co-
198 cultured with EGFRt- but not with S-CAR-expressing target cells (Figure 3B). This
199 indicated a CD8⁺ T-cell response against the human-derived EGFRt. In contrast, we
200 did not detect a CD8⁺ T-cell response against the S-CAR although it also contains
201 human-derived domains, namely the extracellular scFv C8, a human IgG1 spacer, a
202 transmembrane domain from human CD28 and intracellular signaling domains of
203 human CD28 and CD3 ζ .

204 This finding, together with the time kinetics of vanishing S-CAR- or EGFRt-stainings
205 on day 5 or 7, respectively (Figure 3A), indicated an additional immunological
206 mechanism playing a role in S-CAR T-cell rejection. We therefore decided to also
207 test for anti-S-CAR and anti-EGFRt antibodies, incubated our target cells expressing
208 either the S-CAR or EGFRt with mouse sera of recipient mice and stained for bound
209 murine IgG antibodies. Flow cytometry analysis revealed antibody production against
210 both the S-CAR and EGFRt molecules (Figure 3C). To confirm anti-S-CAR
211 antibodies and to investigate which domains of the S-CAR were targeted by the
212 antibodies, an enzyme-linked immunosorbent assay (ELISA) was established. This
213 ELISA confirmed the presence of antibodies against both extracellular domains of the
214 S-CAR, namely the human IgG1 spacer (Figure 3D) and the scFv C8 (Figure 3E).

215 As an attempt to prevent an antibody response against the S-CAR, the number of
216 immunogenic extracellular epitopes was reduced by exchanging the spacer to a
217 murine IgG1 domain (Figure S1) and excluding the EGFRt. The intracellular signaling
218 domains were left unaltered as no T-cell response against the S-CAR had been
219 detected. Thus, in this murine IgG1 S-CAR construct only the human-derived scFv
220 C8 remained as a potentially immunogenic extracellular epitope. To study the effect
221 of an antibody response against the scFv C8, we transferred murine IgG1 S-CAR T
222 cells into HBV-transgenic mice. In murine IgG1 S-CAR T cell-treated mice, numbers
223 of transferred cells declined with kinetics comparable to those in mice treated with S-
224 CAR T cells containing a human IgG1 (Figure 3F). While no anti-hIgG1 antibodies
225 were detected anymore, we still detected antibodies directed against the human-
226 derived scFv C8 domain (Figure 3G).

227 Taken together, the EGFRt elicited B- and T-cell responses in immunocompetent
228 mice, while the S-CAR elicited only antibody responses. Antibody responses were
229 directed against the scFv C8 binder, which is of human origin, as well as the human
230 IgG1 spacer domain within the S-CAR. Since the human scFv binder was also
231 targeted by antibodies, a reduction of immunogenic epitopes did not prevent rejection
232 of S-CAR T cells by the endogenous immune system. Exchanging the scFv,
233 however, does not allow preclinical evaluation of a CAR anymore. Thus, alternative
234 models are required for preclinical evaluation of a human CAR.

235

236 **Irradiation allows long-term persistence of S-CAR T cells**

237 Sublethal total body irradiation is an option to prevent rejection of cells expressing
238 alloantigens.²² To establish tolerance against S-CAR- and EGFRt-expressing T cells

239 in AAV-HBV-infected immunocompetent mice, recipients were irradiated one day
240 before T-cell transfer (Figure 4A). Under this condition, S-CAR T cells expanded and
241 persisted until day 140 in peripheral blood (Figure 4B and C, gating strategy depicted
242 in Figure S5). Importantly, even when B cells and CD8⁺ T cells (Figure 4D) as well as
243 CD4⁺ T cells and NK cells (Figure S6) had reached physiological concentrations
244 again 80 days after irradiation, the concentration of S-CAR T cells remained stable.

245 At day 140 after transfer, S-CAR T cells were still detected at high numbers in liver
246 and spleen (Figure 4E) and allowed characterizing their phenotype. The majority of
247 S-CAR T cells (60-70 %) in both organs exhibited an effector phenotype (CD62L⁻
248 CD127⁻) (Figures 4F and S7A). Mock-transduced CD8⁺ T cells, in contrast, showed a
249 phenotype of naïve or central-memory T cells (CD62L⁺ CD127⁺, 60-70 % in liver, 89-
250 94 % in spleen). When exhaustion markers were analyzed, a high percentage of S-
251 CAR T cells were positive for PD-1 but only about 25 % expressed Tim-3, and CTLA-
252 4 was barely detected at all (Figures 4G and S7B). To investigate the functionality of
253 S-CAR T cells after *in vivo* circulation for more than four months, cells from liver and
254 spleen isolated on day 140 after transfer were re-stimulated *ex vivo* on plate-bound
255 HBsAg. ICS revealed that the transduced S-CAR T cells could still be activated and
256 expressed the proinflammatory cytokines IFN- γ and to a lower extent TNF- α upon
257 antigen encounter (Figure 4H). Furthermore, irradiation prevented the development
258 of anti-human-IgG1 and anti-scFv C8 antibodies upon S-CAR T-cell transfer (Figure
259 4I). In summary, irradiation of immunocompetent mice prior to T-cell transfer allowed
260 expansion and long-term persistence of S-CAR T cells, which developed an effector
261 phenotype and to a considerable proportion remained functional.

262

263 **S-CAR T cells have long-term antiviral function in irradiated,**
264 **immunocompetent mice**

265 Having shown that transferred S-CAR T cells could expand and survive in AAV-HBV-
266 infected and irradiated wildtype mice, we next determined their antiviral effect in this
267 model. Mice that received S-CAR T cells, both with and without prior irradiation,
268 displayed 2- to 4-fold elevated serum ALT levels on day 7 (Figure 5A). Around day
269 40, irradiated mice treated with S-CAR T cells but not the other groups showed a
270 moderate ALT elevation again. Serum HBsAg levels dropped by 1 log₁₀ until day 30
271 in both S-CAR T cell-treated groups independent of prior irradiation. However,
272 HBsAg subsequently rebounded in mice without prior irradiation reaching
273 pretreatment levels again around day 80 (Figure 5B). One mouse (not irradiated)
274 developed spontaneous HBV-immunity >80 days after S-CAR T-cell treatment and
275 seroconverted with a drop in HBsAg of >3 log₁₀ and anti-HBsAg antibodies
276 detectable on day 140 (Figure 5C). In all irradiated and S-CAR T cell-treated mice,
277 HBsAg continued to decrease to <1 % of pretreatment values until day 140 (Figure
278 5B) and HBeAg continuously dropped (Figure 5D). This was not observed in non-
279 irradiated or mock T cell-treated animals. The antiviral effect was confirmed by qPCR
280 analysis of liver DNA. AAV as well as HBV DNA copies in the liver were significantly
281 reduced in irradiated and S-CAR T cell-treated mice compared to the other groups
282 (Figure 5E). Thus, when initiation of immune responses against the human-derived
283 S-CAR was prevented by irradiation, S-CAR T cells expanded, persisted long-term
284 and elicited a significant antiviral effect in AAV-HBV-infected mice. Whether low-level
285 persistence of HBsAg and HBeAg was due to the fact that the observation period
286 was limited to 140 days or to the fact that the largely reduced antigen levels were not
287 sufficient to stimulate the S-CAR anymore cannot be clarified.

288 **S-CAR-specific tolerization of mice allows T-cell persistence and antiviral**
289 **efficacy**

290 To further improve the model and allow S-CAR T-cell transfer into fully
291 immunocompetent animals, we aimed at inducing antigen-specific tolerance to the
292 human-derived CAR domains and EGFRt before S-CAR T-cell transfer. To this end,
293 non-functional S Δ -CAR T cells co-expressing EGFRt were transferred into AAV-
294 HBV-infected mice one day after irradiation (Figure 6A). S Δ -CAR T cells should
295 neither proliferate nor show any effector function in AAV-HBV-infected mice. We
296 hypothesized that the presence of the human alloantigens from S Δ -CAR and EGFRt
297 during recovery of the endogenous immune system would allow to induce specific
298 immune tolerance.

299 As observed before, irradiation of mice induced a depletion of endogenous B- and T-
300 cell populations that were restored in numbers after two months (Figure S8A-C). S Δ -
301 CAR/EGFRt T cells injected at the time of irradiation persisted at low concentration
302 for more than three months (Figure S8D). After three months functional S-CAR T
303 cells that were additionally grafted with EGFRt were injected. Mice that had been
304 irradiated and had received S Δ -CAR T cells neither mounted an antibody response
305 against the human IgG1 or scFv C8 domains of the S-CAR (Figure 6B) nor
306 developed a CD8⁺ T-cell response against the EGFRt (Figure 6C). In contrast, mice
307 only irradiated but not tolerized using S Δ -CAR T cells mounted B- and T-cell
308 responses against the human alloantigens. Functional S-CAR T cells proliferated well
309 and persisted in tolerized mice until the end of the study, i.e. day 110 after S-CAR T-
310 cell transfer (Figure 6D), but rapidly vanished from peripheral blood in mice that had
311 not been tolerized. This shows that functionality of the endogenous immune system

312 against the foreign antigens S-CAR and EGFRt had been re-established after
313 irradiation at the time point when functional S-CAR T cells were transferred. On the
314 other hand, it proves that antigen-specific immune tolerance induced by the S Δ -CAR
315 T-cell transfer after irradiation was sufficient to allow persistence of S-CAR T cells.
316 In the tolerized animals, in which S-CAR T cells expanded and survived, we then
317 determined the antiviral effect of S-CAR T cells. Serum ALT levels remained slightly
318 elevated after S-CAR T-cell treatment, although statistically significant only on day
319 110 (Figure 6E). Viral HBsAg decreased by 2 log₁₀ in tolerized animals, but remained
320 unaltered in the other groups (Figure 6F). Both serum HBeAg levels (Figure 6G) as
321 well as AAV-DNA and HBV-DNA copies in the liver (Figure 6H) decreased about 60
322 % in comparison to control groups. Again, despite being quite efficient, S-CAR T-cell
323 therapy did not fully cure mice from HBV infection and a proportion of HBV-positive
324 hepatocytes persisted.

325

326

327 **DISCUSSION**

328 Appropriate mouse models are needed for thorough preclinical investigations of CAR
329 T-cell products. While a CAR ideally consists of only human-derived domains when
330 applied to a patient, the same construct may be recognized as foreign in
331 immunocompetent mice. Hence, therapeutic efficacy and safety profiles might be
332 altered due to limited CAR T-cell persistence. Here we show that induction of
333 adaptive immunity is indeed an issue when investigating CAR T cells harboring
334 human domains in an immunocompetent mouse model. After initial expansion, HBV-
335 specific S-CAR T-cell numbers rapidly declined and a second S-CAR T-cell transfer

336 was unable to induce an antiviral effect anymore. Cells that express either the CAR
337 or EGFRt as a safeguard, could be used to detect antibodies in serum of treated
338 mice and CD8⁺ T-cell responses via flow cytometry-based assays. These
339 experiments showed that EGFRt was targeted by both humoral and cellular immune
340 responses. While we could only detect humoral immune responses against the S-
341 CAR these were unfortunately at least partially directed against the scFv binder as
342 confirmed by specifically developed ELISAs. The scFv C8 binder as the only
343 essential domain of human origin was still sufficient to induce antibody responses
344 and a loss of S-CAR T cells. The rapid decrease of CAR T cells also occurred in
345 HBV-negative mice, or when CAR T cells lacked signaling domains or harbored a
346 spacer with reduced Fc-receptor binding capacity (Figure S1).²⁰ Hence, we
347 concluded that neither T-cell exhaustion, nor activation induced cell death due to
348 overactivation by antigen or by binding of Fc-receptors to the CAR, could have
349 played a role in reduced S-CAR T-cell persistence.

350 When mice were irradiated directly before T-cell transfer, we were able to induce
351 long-term tolerance to the S-CAR and EGFRt alloantigens with S-CAR T cells being
352 detected at high numbers even 140 days after transfer in peripheral blood, spleen
353 and liver. Since S-CAR T cells were transferred only one day after irradiation, when
354 the immune system was strongly depressed, one could argue that the mice were not
355 fully immunocompetent. Therefore, we investigated if we could induce a specific
356 tolerance to the alloantigens by an immediate transfer of non-functional SΔ-CAR T
357 cells. Although these cells persisted only at low numbers due to a lack of an
358 activation signal, their numbers were sufficient to induce specific tolerance against
359 the human-derived domains, and functional S-CAR T cells were able to persist for

360 more than three months in constantly high numbers and to elicit an antiviral function
361 even when encountering a fully reconstituted immune system.

362 Our results show that a specific immune tolerance has been induced by transfer of
363 the non-functional SΔ-CAR T cells preventing rejection of S-CAR T cells after
364 immune reconstitution. Full reconstitution of the immune system at the time point of
365 S-CAR T cell transfer was indicated since mice that had only been irradiated but did
366 not receive an early transfer of SΔ-CAR T cells rejected the S-CAR T cells. Immune
367 tolerance can be achieved by two distinct means, namely central and peripheral
368 tolerance. We propose that central tolerance is the mode-of-action of tolerance
369 induction to transferred S-CAR T cells.

370 Central tolerance is induced in the thymus when during T-cell development and after
371 T-cell receptor gene rearrangement, T cells are assessed for their specificity.²³ Only
372 T cells with a non-self T-cell receptor specificity can leave the thymus and become
373 part of the pool of mature peripheral T cells. Since auto-reactive T cells are excluded
374 this way, the T-cell pool usually does not target self-tissue and auto-immune
375 diseases remain a rare event.²³ If autoreactive T cells escape negative selection in
376 the thymus or an antigen is only encountered later in life, peripheral tolerance comes
377 into play.²⁴ Tissue damage is prevented by conversion of T cells to Tregs, induction
378 of T-cell apoptosis, T-cell exhaustion or anergy by e.g. metabolic alteration. B cells
379 experience similar selection mechanisms.²⁵ In their case, central tolerance is
380 achieved during maturation in the bone marrow. If autoreactive B cells escape
381 negative selection, absent CD4⁺ T-cell help in the periphery prevents B-cell activation
382 and antibody production.

383 In our setting, the alloantigens expressed on transferred T cells (namely extracellular
384 domains of the S-CAR and the EGFRt) were present during replenishment of the
385 immune cell pool after irradiation. It was previously reported that intrathymic antigen
386 inoculation after total body irradiation can induce selective non-responsiveness to
387 bovine gamma globulin as an alloantigen in rats.²² Similarly, intrathymic
388 transplantation of pancreatic islet allografts after lymphodepletion led to acceptance
389 of islet grafts both in- and outside the thymus.²⁶ Hereby, clonal deletion induced by
390 recognition of alloantigens was identified as mode-of-action for selective non-
391 responsiveness.²⁷ For our case, we propose the following concept of non-
392 responsiveness to the human-derived antigens: adoptively transferred SΔ-CAR T
393 cells are distributed throughout the body and will migrate to the thymus. Here, cross-
394 presentation of peptides by thymic dendritic cells²⁸ induces negative selection for
395 both CD4⁺ and CD8⁺ T cells with specificities for S-CAR or EGFRt epitopes. This
396 would directly prevent CD8⁺ T-cell responses, and indirectly B-cell responses
397 because of a lacking CD4⁺ T-cell help. Our data indicate that the presence of the
398 alloantigens during recovery from total body irradiation deluded the immune system
399 in a way that the human-derived domains are considered self-antigens and must not
400 be targeted.

401 The situation may be comparable to the clinical setting. Murine components of CAR
402 T-cell products have been reported to be immunogenic in humans. Stronger
403 lymphodepleting preconditioning with fludarabine instead of only cyclophosphamide-
404 based regimens lead to improved and sustained engraftment of CAR T cells.
405 However, the mechanism by which fludarabine increased CAR T-cell survival and
406 whether immune responses against murine domains were delayed or prevented

407 remains unclear.¹⁰ It may well be the same mechanism we describe in our mouse
408 model.

409 In our setting, S-CAR T-cell therapy had a sustained antiviral effect without inducing
410 apparent therapy-limiting side effects; however, it was not yet able to “cure” the AAV-
411 HBV infection during the 110 days of treatment. One possible explanation would be
412 an insufficient antigenic stimulation, i.e. that the affinity of the scFv C8 is not high
413 enough to detect low amounts of S protein on the membrane. This has been
414 described for an anti-CD20 CAR.²⁹ Alternatively, S protein may not be present on the
415 membrane in a proportion of hepatocytes. T-cell cytokines can downregulate HBV
416 protein expression^{30, 31} and can even deplete the HBV persistence form^{32, 33} without
417 killing infected cells. This will largely reduce the antigen expression level in HBV-
418 positive cells and prevent elimination by T cells. In a clinical setting this limitation may
419 be overcome if patients were selected for high and homogenous expression of viral
420 proteins on the cell surface of HBV-infected cells or HBV-induced HCC tissue in liver
421 biopsies.

422 A second explanation could be inefficient endogenous bystander immunity targeting
423 HBV in the irradiated mice. Since HBV antigens are also continuously present in high
424 amounts when the immune system recovers from irradiation, clonal deletion resulting
425 in selective non-responsiveness to HBV is possible.²⁷ A third explanation could be
426 the liver micro-environment where the anti-HBV immunity needs to become effective.
427 To preserve integrity of the liver as an essential organ, its microenvironment is
428 particularly prone to allow foreign antigens to escape immunity. This is e.g. exploited
429 by pathogens like HBV, hepatitis C virus or malaria sporozoites that persist in the
430 liver and by this frequently escape immune clearance but also explains the

431 extraordinary tolerance of orthotopic liver transplants.^{34, 35} This may be overcome if
432 the S-CAR T cell-induced antiviral immune response paved the way for endogenous
433 immune cells to fight the infection.

434 For reliable preclinical assessment of T-cell therapies, it seems important that the
435 chosen preclinical model closely reflects the anticipated clinical scenario. In particular
436 if chronic viral infections or particular solid cancers shall be treated, there will be a
437 need to apply CAR T cells without prior immunosuppression although
438 lymphodepletion seems to support CAR T-cell efficacy. As a potential reason for the
439 beneficial effect of lymphodepletion, competition for cytokines with endogenous
440 immune cells but also alteration of the tumor microenvironment or simply a lack of
441 space for the transferred cells to expand have been discussed.³⁶ To fully understand
442 the benefit of lymphodepletion prior to T-cell transfer, orthotopic and immune
443 competent preclinical models are required and will help to improve clinical efficacy of
444 CAR T-cell therapy in settings other than hematological malignancies.³⁷

445 For adoptive T-cell therapy of chronic HBV infection and HBV-associated HCC it is
446 essential to rely on preclinical models using immunocompetent animals as this
447 reflects the clinical situation. For both diseases, lymphodepleting regimes are
448 contraindicated. Several studies have reported that chemotherapy in chronic HBV
449 carriers leads to virus reactivation.³⁸⁻⁴⁰ Especially lymphodepletion via
450 cyclophosphamide, which is commonly used before T-cell transfer, leads to
451 reactivation of HBV in up to one third of patients.⁴¹ Already the depletion of B cells
452 using anti-CD20 antibodies results in life-threatening HBV reactivation.⁴² Therefore,
453 preclinical evaluation of S-CAR T-cell therapy in an immunocompetent rather than an

454 immunocompromised mouse model is needed, since it is likely to provide an efficacy
455 and safety profile that has relevance for clinical application.

456 Importantly, the model described here is transferable to other CAR T-cell
457 approaches, e.g. the treatment of solid tumors, that shall be evaluated in
458 immunocompetent preclinical models and utilize human scFv. In comparison to
459 models using immunodeficient mice, the tolerized animals offer the advantage that
460 they have a fully functional immune system at the time of CAR T-cell transfer
461 allowing to investigate interactions with and activation of the endogenous immune
462 system and how this influences efficacy and safety of the therapy. Tumor infiltration
463 by bystander immune cells will certainly contribute to an anti-tumor response but
464 potentially also to a cytokine storm.³⁷ To evaluate all consequences of a cytokine
465 storm, cytokine receptors matching between transferred T cells and host tissue are
466 required as it is the case in our model. Furthermore, in this model a combination
467 therapy with checkpoint inhibitors targeting CAR T cells but also endogenous
468 immune cells can be evaluated.

469 The model described here is the only model that allows studying a CAR with human-
470 derived domains in the context of an intact immune system besides humanized
471 mouse models harboring human immune cells. In contrast to humanized mouse
472 models, our model allows to transfer syngeneic murine T cells which is of special
473 importance for long-term studies of cell-cell interactions and to avoid
474 misinterpretation of anti-tumor efficacy by graft-versus-host reactions.⁴³ Compared to
475 humanized mouse models, our model is less laborious, cheaper and more
476 physiological.

477 Taken together, by irradiation and subsequent tolerization with a signaling-deficient
478 CAR, we were able to induce long-lasting, specific tolerance to human-derived CAR
479 domains, and could study the engraftment, proliferation, long-term persistence and
480 antiviral effector function of S-CAR T cells in fully immunocompetent mice. We
481 believe that this model can be transferred to other CAR T-cell approaches in case
482 they require preclinical evaluation in the context of a fully functional immune system.
483 It will allow for the study of interactions with the different arms of the endogenous
484 immune system, bystander immune cell activation and combination therapies with
485 checkpoint inhibitors. Thus, it will help to bring better characterized, more efficient
486 and safer cell products into the clinics.

487

488 **MATERIALS AND METHODS**

489

490 Animal models

491 HBVtg HBV1.3xfs mice (HBV genotype D, serotype *ayw*), Rag2^{-/-} mice, Rag2^{-/-}/IL-
492 2Rγ^{-/-} mice, and CD45.1⁺ C57BL/6 donor mice were bred in-house in specific
493 pathogen-free animal facilities. Adeno-associated virus (AAV) serotype 2 containing
494 the 1.2 overlength genome of HBV genotype D (AAV-HBV) was packed with an AAV
495 serotype 8 capsid as previously described.²¹ Viral vector was produced by
496 Plateforme de Thérapie Génique (Nantes, France). For the AAV-HBV model, 8-
497 week-old male wildtype C57BL/6J mice were purchased from Janvier (Le Genest-
498 Sain-Isle, France) and infected with 2 x 10¹⁰ viral particles 3-4 weeks before T-cell
499 transfer. The study was conducted according to the German Law for the Protection of
500 Animals.

501 Retroviral transduction and adoptive T-cell transfer

502 Splenocytes were isolated from donor mice and enriched for CD8⁺ T cells using
503 CD8a MACS beads (Miltenyi Biotec, Bergisch Gladbach, Germany). A total of 1.5 x
504 10⁶ CD8⁺ T cells/well were stimulated for 24 hours with 5 ng/ml IL-12 (kindly provided
505 by E. Schmitt, University of Mainz) on tissue-treated 12-well plates that were
506 precoated with anti-CD3 and anti-CD28 antibodies (kindly provided by R. Feederle,
507 Helmholtz Zentrum München) for 2 hours at 37 °C (10 µg/ml in PBS). The next day,
508 cells were transferred to uncoated 12-well plates and retrovirally transduced two days
509 in a row. Retroviral supernatants were obtained from Platinum-E packaging cells
510 transfected with MP71 retroviral plasmids containing CAR coding sequences.
511 Activated CD8⁺ T cells and retroviral supernatants were supplemented with 2 µg/ml
512 protamine sulfate (Leo Pharma, Neu-Isenburg, Germany) and spinoculated (850 x g,
513 32 °C, 2 hours). The day after the second transduction, cells were analyzed by flow
514 cytometry and the transduction rate determined as described below. Cells were
515 washed twice with PBS, resuspended in PBS and transferred intraperitoneally in 200
516 µl into mice that were grouped by HBsAg and HBeAg levels. If applicable, mice were
517 irradiated with 5 Gray one day before T-cell transfer.

518 Isolation of splenocytes, liver-associated lymphocytes and peripheral blood
519 mononuclear cells

520 Spleens were mashed through a 100 µm cell strainer and erythrocytes lysed using
521 ACK lysis buffer (8 g NH₄Cl, 1 g KHCO₃, 37 mg Na₂EDTA, add to 1 l H₂O, pH 7.2-
522 7.4) for 2 min at RT. Livers were perfused with PBS to eliminate circulating
523 lymphocytes in blood and mashed through a 100 µm cell strainer. Mashed liver tissue
524 was digested with 4500 U collagenase type 4 (Worthington, Lakewood, USA) (20

525 min, 37 °C) and leukocytes were purified in an 80 %/40 % Percoll (GE Healthcare,
526 Solingen, Germany) gradient (1400 x g, 20 min, RT, without brake). For peripheral
527 blood mononuclear cell isolation, peripheral blood was collected into Microvette 500
528 LH-Gel tubes (Sarstedt, Nümbrecht, Germany) and 15 µl of blood was incubated with
529 250 µl ACK lysis buffer for 2 min at RT, and then resuspended in fluorescence-
530 activated cell sorting (FACS) buffer (0.1 % bovine serum albumin in PBS).

531 Flow cytometry

532 Staining of cells was performed for 30 min in the dark on ice in FACS buffer (0.1 %
533 bovine serum albumin in PBS). Antibodies were purchased from different suppliers:
534 CD4, CD8, CD19, CD45.1, IFN-γ, TNF-α (BD Biosciences, Heidelberg, Germany);
535 CD3, CD45.2, CD62L, CD127, NK1.1, PD-1 (Thermo Fisher Scientific, Germering,
536 Germany); CTLA-4, Tim-3 (Biolegend, Koblenz, Germany). Viable cells were
537 determined with live/dead cell marker (Thermo Fisher Scientific). For intracellular
538 cytokine staining cells were permeabilized using Cytofix/Cytoperm (BD Biosciences)
539 prior to incubation with antibodies following manufacturer's instruction. Total cell
540 numbers were determined by the addition of CountBright™ Absolute Counting Beads
541 (Thermo Fisher Scientific). Cells were analyzed on a FACS Canto II (BD
542 Biosciences) or CytoFLEX S (Beckman Coulter, Munich, Germany). If a CAR, EGFRt
543 and other surface markers were analyzed, first the CAR was stained with an anti-
544 human-IgG (Abcam, Cambridge, UK) or anti-murine-IgG (BD Biosciences) antibody,
545 followed by the primary staining of EGFRt with biotin-labelled cetuximab (Merck,
546 Darmstadt, Germany). In a last step, bound cetuximab was stained with
547 fluorochrome-labelled streptavidin (Thermo Fisher Scientific) together with additional
548 antibodies against surface markers.

549 Cultivation of murine cells

550 Primary murine cells were cultured in murine T-cell medium (RPMI Dutch modified,
551 10 % FCS, 1 % glutamine, 1 % Pen/Strep, 1 % sodium pyruvate and 50 μ M β -
552 mercaptoethanol; Thermo Fisher Scientific).

553 Ex vivo T-cell stimulation

554 Functionality of S-CAR T cells was determined by culturing 5×10^5 splenocytes or
555 liver-associated lymphocytes/well on tissue-treated 96-well plates precoated with
556 HBsAg (2.5 μ g/ml in PBS, overnight, 4 °C; Roche Diagnostics, Mannheim, Germany)
557 or anti-CD3 and anti-CD28 antibodies (10 μ g/ml in PBS, overnight, 4 °C). To
558 determine an immune response against the S-CAR and EGFRt, 1×10^6 splenocytes
559 were cultured with 1×10^5 S-CAR⁺ or EGFRt⁺ CD8⁺ T cells. After 1 hour of culture, 1
560 μ g/ml Brefeldin A (Sigma-Aldrich, Munich, Germany) was added. Cytokine
561 expression was determined the following day via an intracellular cytokine staining
562 and flow cytometry analysis.

563 Cell-based anti-S-CAR and anti-EGFRt antibody detection

564 Platinum-E cells were transfected with MP71 plasmids encoding the S-CAR or
565 EGFRt. After 48 hours, cells were harvested, and a flow cytometry staining was
566 performed. Cells were stained with serum diluted 1:200 in FACS buffer and in a
567 subsequent staining step incubated with PE-labeled anti-mouse-IgG antibody (12-
568 4010-82; Thermo Fisher Scientific). Median fluorescence intensity was determined
569 on a CytoFLEX S (Beckman Coulter).

570 ELISA-based anti-C8 and anti-IgG1 antibody detection

571 ELISA plates were precoated overnight with recombinant scFv C8 (1 µg/ml in PBS)
572 or IgG1 cetuximab antibody (1 µg/ml in PBS; Merck) at 4 °C. The next day, plates
573 were blocked with assay diluent (1 % bovine serum albumin in PBS) for 1 hour at RT.
574 Diluted serum of treated mice was incubated on wells for 2 hours and bound
575 antibodies were detected with an HRP-labelled anti-mouse-IgG antibody (1:1000,
576 Sigma-Aldrich). TMB substrate (Thermo Fisher Scientific) conversion (OD₄₅₀ nm -
577 OD₅₆₀ nm) was measured on an infinite F200 photometer (Tecan, Männedorf,
578 Switzerland) and the signal of serum on uncoated wells subtracted.

579 Intrahepatic AAV and HBV DNA copies

580 DNA was extracted from approximately 20 mg of liver issue using the Nucleo Spin
581 Tissue Kit (Macherey-Nagel, Berlin, Germany) following manufacturer's instructions.
582 Quantitative PCR was performed with SyBrGreen (Roche Diagnostics) on a
583 LightCycler® 480 II (Roche Diagnostics) using the following primers: AAVfw:
584 AACCCGCCATGCTACTTATCTACGT; AAVrev: CACACAGTCTTTGAAGTAGGCC;
585 HBVfw: GCCTCATCTTCTTGTTGGTTC; HBVrev:
586 GAAAGCCCTACGAACCACTGAAC. Results were normalized to cell numbers using
587 the single copy gene *PRNP*: PRNPfw: TGCTGGGAAGTGCCATGAG; PRNPrev:
588 CGGTGCATGTTTTTCACGATAGTA.

589 Serological analyses

590 Peripheral blood was collected into Microvette 500 LH-Gel tubes (Sarstedt) and
591 centrifuged to separate serum (10 min, 5000 x g, RT). ALT activity was determined
592 1:4 diluted with PBS using the Reflotron ALT test (Roche Diagnostics). Serum
593 HBsAg, HBeAg and anti-HBsAg antibody were quantified in different dilutions with
594 PBS on an Architect™ platform using the quantitative HBsAg test (Ref.: 6C36-44;

595 Cutoff: 0.25 IU/ml), the HBeAg Reagent Kit (Ref.: 6C32-27) with HBeAg Quantitative
596 Calibrators (Ref.: 7P24-01; Cutoff: 0.20 PEI U/ml) and the anti-HBs test (Ref.: 7C18-
597 27; Cutoff: 12.5 mIU/ml) (Abbott Laboratories, Wiesbaden, Germany).

598 Production of recombinant scFv C8

599 *E. coli* XL1-blue were transformed with scFv C8-encoding pHOG21 plasmid and a
600 single clone colony inoculated overnight in 5 ml LB media (10 g Tryptone, 5 g yeast
601 extract, 10 g NaCl, add to 1 l H₂O). The next day, 3 l of 2x YT (17 g Tryptone, 10 g
602 yeast extract, 5 g NaCl, add to 1 l H₂O) were inoculated 1:1000 and grown for
603 approximately 10 hours until the OD₆₀₀ reached 0.6. Induction was performed
604 overnight at 18 °C with 0.1 mM IPTG (Carl Roth, Karlsruhe, Germany). Large-scale
605 protein purification was performed by fast protein liquid chromatography under native
606 conditions on an ÄKTA avant (GE Healthcare). Bacterial cells of the overnight
607 induction culture were harvested (15 min, 5000 x g, RT) and resuspended in 10 ml
608 ÄKTA binding buffer (20 mM disodium phosphate, 500 mM NaCl, 20 mM imidazole,
609 pH 7.4) per 1 g of bacterial pellet. 3 U/ml benzonase (Merck) and 0.2 mg/ml
610 lysozyme (Thermo Fisher Scientific) were added, followed by incubation for 20 min
611 on ice. The samples were then submitted to five cycles of sonication 1 min each, and
612 centrifuged (30 min, 5000 x g, 4 °C). Samples were continuously kept on ice.

613 A HisTrap™ FF crude 5 ml column (GE Healthcare) was connected to the ÄKTA
614 avant (GE Healthcare) and loaded with lysate. Samples were eluted by gradually
615 increasing the proportion of elution buffer (20 mM disodium phosphate, 500 mM
616 NaCl, 500 mM imidazole, pH 7.4) with at flow rate of 5 ml/min collecting 1 ml
617 fractions. The protein content of the eluent was measured by UV monitoring at 280
618 nm. According to the chromatographic peaks, the respective fractions were analyzed

619 by SDS-PAGE and Coomassie staining in order to confirm protein presence. Positive
620 fractions were pooled and dialyzed to storage buffer (25 mM Tris-HCl, 100 mM KCl, 1
621 mM EDTA, 1 mM MgCl₂, 10 % Glycerol, pH 7.4) overnight at 4 °C. The final sample
622 was filtered and protein concentration was measured via a Nanodrop One (Thermo
623 Fisher Scientific).

624

625 **AUTHOR CONTRIBUTIONS**

626 MMF, JF, TA and KW conducted the experiments; SS and JS produced critical
627 reagents and helped to perform experiments; SPF helped with experimental set-up
628 and performed irradiation; DHB provided essential infrastructure and technical
629 support; MMF, KW, MMH and UP designed the experiments; MMF, KW and UP
630 wrote the paper.

631

632 **CONFLICT OF INTEREST**

633 The work was funded by the German Research Foundation (DFG) via TRR36 and
634 the German Center for Infection Research (DZIF). UP and KW are co-founders of
635 and MF was part-time employed by SCG Cell Therapy, Singapore. KW is consulting
636 for LION TCR / SCG Cell Therapy, Singapore. UP serves as ad-hoc scientific advisor
637 for Roche, GILEAD; J&J, Abbvie, Merck, Arbutus and VIR Biotechnology.

638

639 **ACKNOWLEDGMENTS**

640 We are grateful to Michael Jensen for providing the EGFRt construct, Hinrich Abken
641 for providing CAR constructs, and Marie-Louise Michel for providing the AAV-HBV1.2
642 construct. We thank Philipp Hagen, Natalie Röder and Romina Bester for excellent
643 technical assistance and Claudia Dembek for critical reading of the manuscript.

644

645 REFERENCES

- 646 1. Gill, S., Maus, M.V., and Porter, D.L. (2016). Chimeric antigen receptor T cell therapy: 25
647 years in the making. *Blood reviews* 30: 157-167.
- 648 2. Brower, V. (2017). First Chimeric Antigen Receptor T-Cell Therapy Approved. *J Natl*
649 *Cancer Inst* 109.
- 650 3. Mullard, A. (2017). Second anticancer CAR T therapy receives FDA approval. *Nat Rev*
651 *Drug Discov* 16: 818.
- 652 4. Hartmann, J., Schüßler- Lenz, M., Bondanza, A., and Buchholz, C.J. (2017). Clinical
653 development of CAR T cells—challenges and opportunities in translating innovative
654 treatment concepts. *EMBO molecular medicine*: e201607485.
- 655 5. Bohne, F., Chmielewski, M., Ebert, G., Wiegmann, K., Kurschner, T., Schulze, A., *et al.*
656 (2008). T cells redirected against hepatitis B virus surface proteins eliminate infected
657 hepatocytes. *Gastroenterology* 134: 239-247.
- 658 6. Full, F., Lehner, M., Thonn, V., Goetz, G., Scholz, B., Kaufmann, K.B., *et al.* (2010). T
659 cells engineered with a cytomegalovirus-specific chimeric immunoreceptor. *J Virol* 84:
660 4083-4088.
- 661 7. Sautto, G.A., Wisskirchen, K., Clementi, N., Castelli, M., Diotti, R.A., Graf, J., *et al.*
662 (2016). Chimeric antigen receptor (CAR)-engineered T cells redirected against hepatitis
663 C virus (HCV) E2 glycoprotein. *Gut* 65: 512-523.
- 664 8. Hale, M., Mesojednik, T., Romano Ibarra, G.S., Sahni, J., Bernard, A., Sommer, K., *et al.*
665 (2017). Engineering HIV-Resistant, Anti-HIV Chimeric Antigen Receptor T Cells.
666 *Molecular therapy : the journal of the American Society of Gene Therapy* 25: 570-579.
- 667 9. Leibman, R.S., Richardson, M.W., Ellebrecht, C.T., Maldini, C.R., Glover, J.A., Secreto,
668 A.J., *et al.* (2017). Supraphysiologic control over HIV-1 replication mediated by CD8 T

- 669 cells expressing a re-engineered CD4-based chimeric antigen receptor. PLoS pathogens
670 13: e1006613.
- 671 10. Turtle, C.J., Hanafi, L.A., Berger, C., Gooley, T.A., Cherian, S., Hudecek, M., *et al.*
672 (2016). CD19 CAR-T cells of defined CD4+:CD8+ composition in adult B cell ALL
673 patients. J Clin Invest 126: 2123-2138.
- 674 11. Siegler, E.L., and Wang, P. (2018). Preclinical Models in Chimeric Antigen Receptor-
675 Engineered T-Cell Therapy. Human gene therapy 29: 534-546.
- 676 12. Hay, K.A., and Turtle, C.J. (2017). Chimeric Antigen Receptor (CAR) T Cells: Lessons
677 Learned from Targeting of CD19 in B-Cell Malignancies. Drugs 77: 237-245.
- 678 13. WHO (2017). Hepatitis B, Fact sheet, Updated July 2017 [http://www.who.int/en/news-](http://www.who.int/en/news-room/fact-sheets/detail/hepatitis-b)
679 [room/fact-sheets/detail/hepatitis-b](http://www.who.int/en/news-room/fact-sheets/detail/hepatitis-b).
- 680 14. Sartorius, K., Sartorius, B., Aldous, C., Govender, P.S., and Madiba, T.E. (2015). Global
681 and country underestimation of hepatocellular carcinoma (HCC) in 2012 and its
682 implications. Cancer Epidemiol 39: 284-290.
- 683 15. Gehring, A., and Protzer, U. (2019). Targeting Innate and Adaptive Immune Responses
684 to Cure Chronic HBV Infection. Gastroenterology, in press (ePub ahead of print).
- 685 16. Safaie, P., Poongkunran, M., Kuang, P.P., Javaid, A., Jacobs, C., Pohlmann, R., *et al.*
686 (2016). Intrahepatic distribution of hepatitis B virus antigens in patients with and without
687 hepatocellular carcinoma. World journal of gastroenterology 22: 3404-3411.
- 688 17. Krebs, K., Bottinger, N., Huang, L.R., Chmielewski, M., Arzberger, S., Gasteiger, G., *et*
689 *al.* (2013). T cells expressing a chimeric antigen receptor that binds hepatitis B virus
690 envelope proteins control virus replication in mice. Gastroenterology 145: 456-465.
- 691 18. Wang, X., Chang, W.C., Wong, C.W., Colcher, D., Sherman, M., Ostberg, J.R., *et al.*
692 (2011). A transgene-encoded cell surface polypeptide for selection, in vivo tracking, and
693 ablation of engineered cells. Blood 118: 1255-1263.
- 694 19. Paszkiewicz, P.J., Frassle, S.P., Srivastava, S., Sommermeyer, D., Hudecek, M.,
695 Drexler, I., *et al.* (2016). Targeted antibody-mediated depletion of murine CD19 CAR T
696 cells permanently reverses B cell aplasia. J Clin Invest 126: 4262-4272.
- 697 20. Hombach, A., Hombach, A.A., and Abken, H. (2010). Adoptive immunotherapy with
698 genetically engineered T cells: modification of the IgG1 Fc 'spacer' domain in the
699 extracellular moiety of chimeric antigen receptors avoids 'off-target' activation and
700 unintended initiation of an innate immune response. Gene therapy 17: 1206-1213.

- 701 21. Dion, S., Bourguine, M., Godon, O., Levillayer, F., and Michel, M.L. (2013). Adeno-
702 associated virus-mediated gene transfer leads to persistent hepatitis B virus replication
703 in mice expressing HLA-A2 and HLA-DR1 molecules. *J Virol* 87: 5554-5563.
- 704 22. Staples, P.J., Gery, I., and Waksman, B.H. (1966). Role of the thymus in tolerance: III.
705 Tolerance to bovine gamma globulin after direct injection of antigen into the shielded
706 thymus of irradiated rats. *Journal of Experimental Medicine* 124: 127-139.
- 707 23. Starr, T.K., Jameson, S.C., and Hogquist, K.A. (2003). Positive and negative selection of
708 T cells. *Annu Rev Immunol* 21: 139-176.
- 709 24. Mueller, D.L. (2010). Mechanisms maintaining peripheral tolerance. *Nat Immunol* 11: 21-
710 27.
- 711 25. Nemazee, D. (2017). Mechanisms of central tolerance for B cells. *Nat Rev Immunol* 17:
712 281-294.
- 713 26. Posselt, A.M., Barker, C.F., Tomaszewski, J.E., Markmann, J.F., Choti, M.A., and Naji,
714 A. (1990). Induction of donor-specific unresponsiveness by intrathymic islet
715 transplantation. *Science* 249: 1293-1295.
- 716 27. Turvey, S.E., Hara, M., Morris, P.J., and Wood, K.J. (1999). Mechanisms of tolerance
717 induction after intrathymic islet injection: determination of the fate of alloreactive
718 thymocytes. *Transplantation* 68: 30-39.
- 719 28. Proietto, A.I., Lahoud, M.H., and Wu, L. (2008). Distinct functional capacities of mouse
720 thymic and splenic dendritic cell populations. *Immunology and cell biology* 86: 700-708.
- 721 29. Watanabe, K., Terakura, S., Martens, A.C., van Meerten, T., Uchiyama, S., Imai, M., *et*
722 *al.* (2015). Target antigen density governs the efficacy of anti-CD20-CD28-CD3 zeta
723 chimeric antigen receptor-modified effector CD8+ T cells. *Journal of immunology*
724 (Baltimore, Md : 1950) 194: 911-920.
- 725 30. Guidotti, L.G., Ishikawa, T., Hobbs, M.V., Matzke, B., Schreiber, R., and Chisari, F.V.
726 (1996). Intracellular inactivation of the hepatitis B virus by cytotoxic T lymphocytes.
727 *Immunity* 4: 25-36.
- 728 31. Guidotti, L.G., Rochford, R., Chung, J., Shapiro, M., Purcell, R., and Chisari, F.V. (1999).
729 Viral clearance without destruction of infected cells during acute HBV infection. *Science*
730 284: 825-829.

- 731 32. Lucifora, J., Xia, Y., Reisinger, F., Zhang, K., Stadler, D., Cheng, X., *et al.* (2014).
732 Specific and nonhepatotoxic degradation of nuclear hepatitis B virus cccDNA. *Science*
733 *343*: 1221-1228.
- 734 33. Xia, Y., Stadler, D., Lucifora, J., Reisinger, F., Webb, D., Hosel, M., *et al.* (2016).
735 Interferon-gamma and Tumor Necrosis Factor-alpha Produced by T Cells Reduce the
736 HBV Persistence Form, cccDNA, Without Cytolysis. *Gastroenterology* *150*: 194-205.
- 737 34. Protzer, U., Maini, M.K., and Knolle, P.A. (2012). Living in the liver: hepatic infections.
738 *Nat Rev Immunol* *12*: 201-213.
- 739 35. Knolle, P.A., and Thimme, R. (2014). Hepatic immune regulation and its involvement in
740 viral hepatitis infection. *Gastroenterology* *146*: 1193-1207.
- 741 36. Berger, C., Turtle, C.J., Jensen, M.C., and Riddell, S.R. (2009). Adoptive transfer of
742 virus-specific and tumor-specific T cell immunity. *Curr Opin Immunol* *21*: 224-232.
- 743 37. Srivastava, S., and Riddell, S.R. (2018). Chimeric Antigen Receptor T Cell Therapy:
744 Challenges to Bench-to-Bedside Efficacy. *Journal of immunology (Baltimore, Md : 1950)*
745 *200*: 459-468.
- 746 38. Cheng, J.C., Liu, M.C., Tsai, S.Y., Fang, W.T., Jer-Min Jian, J., and Sung, J.L. (2004).
747 Unexpectedly frequent hepatitis B reactivation by chemoradiation in postgastrectomy
748 patients. *Cancer* *101*: 2126-2133.
- 749 39. Lok, A.S., Liang, R.H., Chiu, E.K., Wong, K.L., Chan, T.K., and Todd, D. (1991).
750 Reactivation of hepatitis B virus replication in patients receiving cytotoxic therapy. Report
751 of a prospective study. *Gastroenterology* *100*: 182-188.
- 752 40. Nakamura, Y., Motokura, T., Fujita, A., Yamashita, T., and Ogata, E. (1996). Severe
753 hepatitis related to chemotherapy in hepatitis B virus carriers with hematologic
754 malignancies. Survey in Japan, 1987-1991. *Cancer* *78*: 2210-2215.
- 755 41. Ma, B., Yeo, W., Hui, P., Ho, W.M., and Johnson, P.J. (2002). Acute toxicity of adjuvant
756 doxorubicin and cyclophosphamide for early breast cancer—a retrospective review of
757 Chinese patients and comparison with an historic Western series. *Radiotherapy and*
758 *oncology* *62*: 185-189.
- 759 42. Perceau, G., Diris, N., Estines, O., Derancourt, C., Levy, S., and Bernard, P. (2006).
760 Late lethal hepatitis B virus reactivation after rituximab treatment of low-grade cutaneous
761 B-cell lymphoma. *Br J Dermatol* *155*: 1053-1056.

762 43. Shultz, L.D., Brehm, M.A., Garcia-Martinez, J.V., and Greiner, D.L. (2012). Humanized
763 mice for immune system investigation: progress, promise and challenges. *Nat Rev*
764 *Immunol* 12: 786-798.

765

766

767 **FIGURE LEGENDS**

768 **Figure 1: Sequential transfers of S-CAR T cells into HBV-transgenic mice. A)**

769 Scheme of the experimental procedure. CD45.2⁺ HBV-transgenic mice were
770 injected once (day 20, grey symbols) or twice (day 0 and day 20, black symbols)
771 with 4×10^6 CD45.1⁺ S-CAR⁺ T cells each (n=7 per group). Transferred, CD45.1⁺
772 cells in peripheral blood and serum parameters were monitored over time. **B)**
773 Numbers of CD45.1⁺ T cells per μ l peripheral blood, **C)** numbers of S-CAR⁺ T cells
774 in peripheral blood and **D)** ALT activity in sera at indicated time points. **E)**
775 Lymphocytes were isolated from liver and spleen on day 33 and cultured on
776 HBsAg- or anti-CD3/anti-CD28- or PBS-coated control plates overnight. Activation
777 of CD45.1⁺ T cells was determined by intracellular staining or IFN- γ and TNF- α
778 followed by flow cytometry analysis. B, C, D: Data points represent individual
779 animals, mean values \pm SD are indicated. E: Data are given as mean values \pm SD.
780 ns = not significant, * = p<0.05, ** = p<0.01, *** = p<0.001 (Mann Whitney test).

781

782 **Figure 2: S-CAR T-cell engraftment in immunocompetent and**

783 **immunodeficient mice.** 2.7×10^6 CD45.1⁺ S-CAR⁺/EGFRt⁺, Δ S-CAR⁺/EGFRt⁺ or
784 mock T cells were transferred into HBV-naïve CD45.2⁺ wildtype C57BL/6J (n=5
785 per group) or Rag2^{-/-} mice (n=3 per group). **A)** CAR and EGFRt expression on
786 CD8⁺ T cells determined by flow cytometry at day of transfer. **B)** Numbers of

787 transferred CD45.1⁺ cells in peripheral blood were determined over time by flow
788 cytometry. **C)-F)** AAV-HBV-infected CD45.2⁺ Rag2^{-/-}/IL-2Rγ^{-/-} mice received 1 x
789 10⁶ S-CAR⁺/EGFRt⁺ T cells each (n=5, grey triangles) or remained untreated (n=3,
790 open triangles). CD45.1⁺ cells in peripheral blood and serum parameters were
791 monitored over time. **C)** Numbers of S-CAR⁺ or EGFRt⁺ cells per μl blood, **D)**
792 serum ALT activity, **E)** HBsAg and **F)** HBeAg levels were determined. All data are
793 given as mean values ± SD. ns = not significant, * = p<0.05 (Mann Whitney test).

794

795 **Figure 3: B- and T-cell responses against S-CAR and EGFRt after T-cell**
796 **transfer. A)-E)** 2.7 x 10⁶ CD45.1⁺ S-CAR⁺/ EGFRt⁺ CD8⁺ T cells were transferred
797 into CD45.2⁺ HBV-naïve wildtype (wt, mock = open circles, S-CAR = black boxes,
798 n=5 per group) or Rag2^{-/-} mice (S-CAR = grey boxes, n=3) (see also Fig. 2B). **A)**
799 Surface expression levels of S-CAR and EGFRt were determined by median
800 fluorescence intensity (MFI) on CD45.1⁺ CD8⁺ T cells in peripheral blood at indicated
801 time points after transfer. **B)** Splenocytes were isolated from treated wt mice on day
802 18 post transfer and co-cultured overnight with mock, S-CAR or EGFRt-expressing
803 CD8⁺ T cells. IFN-γ expression by endogenous CD45.2⁺ CD8⁺ T cells was
804 determined via ICS. **C)** Detection of S-CAR- and EGFRt-specific antibodies in serum
805 of mice on day 18 post transfer. Binding of antibodies to S-CAR- or EGFRt-
806 expressing target cells was determined via bound fluorochrome-labeled secondary
807 anti-mouse IgG antibody by flow cytometry. **D)** Detection of anti-hIgG1 or **E)** anti-
808 scFv C8 antibodies in serial dilutions of mouse sera from day 3 or day 18 post
809 transfer by ELISA. **F)-G)** 2 x 10⁶ CD45.1⁺ T cells expressing an S-CAR with either
810 human (n=3, black boxes) or murine IgG1 spacer domains (n=4, grey triangles) were
811 transferred into CD45.2⁺ HBV-transgenic mice. **F)** Numbers of transferred, CD45.1⁺

812 cells per μl peripheral blood. **G)** Detection of anti-hlgG1 or anti-scFv C8 antibodies in
813 1:200 diluted mouse sera from day 26 by ELISA. A, D, E: Data are given as mean
814 values \pm SD. B, C, F, G: Data points represent individual animals, mean values are
815 indicated (in B, C and F \pm SD). ns = not significant, ** = $p < 0.01$ (Mann Whitney test).

816

817 **Figure 4: S-CAR T-cell engraftment in irradiated mice. A)** Scheme of the
818 experimental procedure. AAV-HBV-infected CD45.2⁺ wildtype mice were injected
819 with 1×10^6 CD45.1⁺ S-CAR⁺/EGFRt⁺ or mock T cells per animal one day after
820 sublethal total body irradiation (S-CAR = black boxes, mock = open circles), or
821 without prior irradiation (S-CAR = grey triangles) (n=4 per group). **B)** Exemplary flow
822 cytometry plot of (transferred) CD45.1⁺ and (endogenous) CD45.1⁻ CD8⁺ T cells in
823 peripheral blood on day 28. **C)** The amount of S-CAR⁺ or EGFRt⁺ T cells per μl
824 peripheral blood was determined by flow cytometry at indicated time points. **D)**
825 Amount of (endogenous) CD45.1⁻ CD19⁺ B cells (left panel) or CD8⁺ T cells (right
826 panel) in peripheral blood. Arrows mark time point of irradiation. **E)** Count of S-CAR⁺
827 or EGFRt⁺ cells in liver and spleen on day 140. **F)** Phenotype of CD8⁺ T-cell subsets
828 of transferred CD45.1⁺ T cells in irradiated mice determined by flow cytometry after
829 staining for CD62L and CD127: effector (CD62L⁻ CD127⁻), effector memory (CD62L⁻
830 CD127⁺), intermediate (CD62L⁺ CD127⁻), naïve / central memory (CD62L⁺ CD127⁺).
831 **G)** Expression of exhaustion markers (PD-1, CTLA-4, Tim-3) on CD45.1⁺
832 lymphocytes isolated from liver and spleen of irradiated mice on day 140. **H)** *Ex vivo*
833 functionality of S-CAR T cells of irradiated mice determined by overnight culture on
834 plate-bound HBsAg or PBS as control. ICS for IFN- γ and TNF- α . **I)** Sera from days -
835 8, 14 and 140 were analyzed by ELISA for anti-hlgG1 and anti-scFv C8 antibodies.
836 C, D, F, H: Data are given as mean values \pm SD. E, G, I: Data points represent

837 individual animals, mean values \pm SD are indicated. Dotted line represents the
838 background determined in mock T cell-treated mice. * = $p < 0.05$ (Mann Whitney test).

839

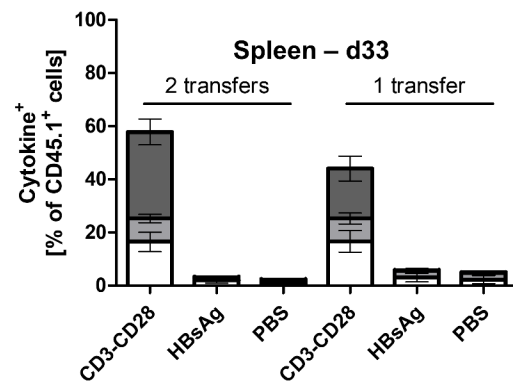
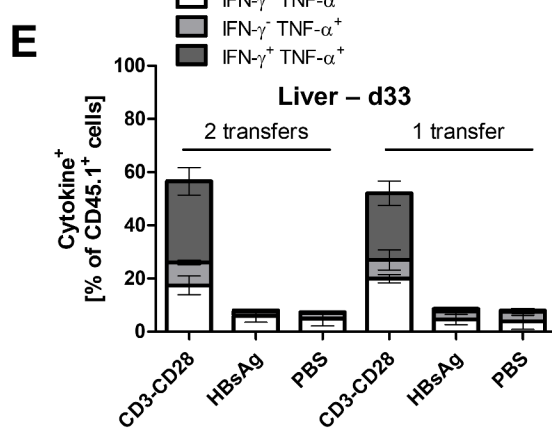
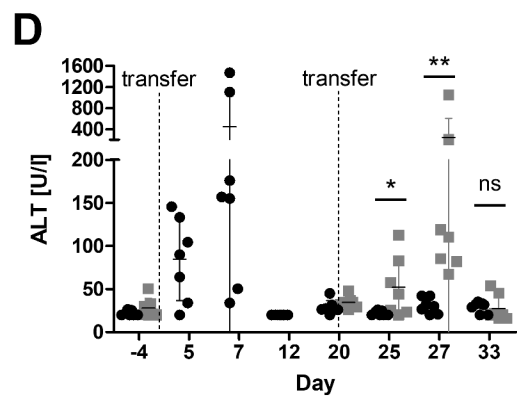
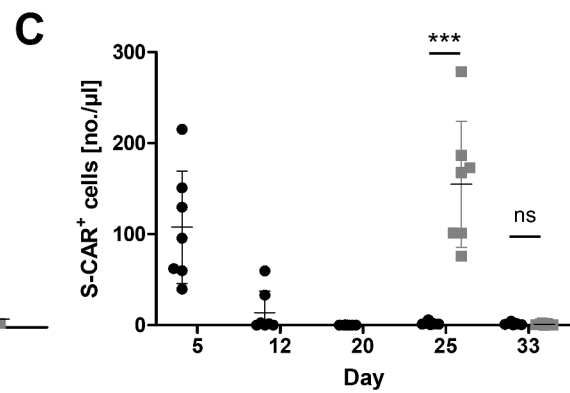
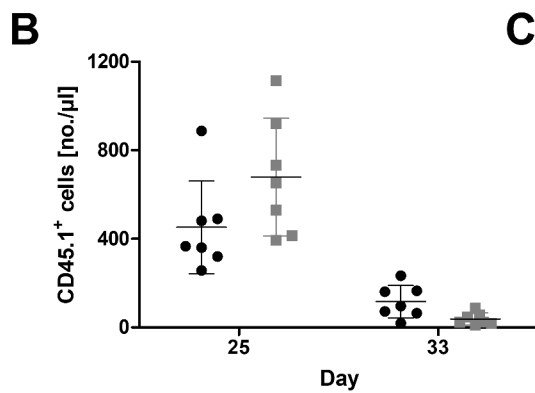
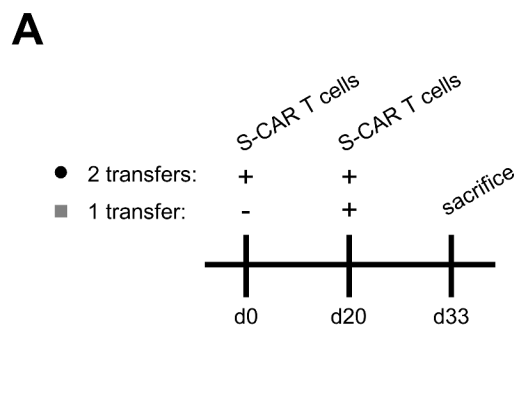
840 **Figure 5: Antiviral effect of S-CAR T cells in irradiated mice.** Identical
841 experimental set-up as in Figure 4. **A)** ALT activity and **B)** HBsAg levels in serum
842 over time. **C)** Inverse correlation of HBsAg and anti-HBsAg antibody concentrations
843 in a single mouse that underwent spontaneous seroconversion. This animal was
844 excluded from B). **D)** HBeAg levels in serum over time. **E)** Intrahepatic AAV- and
845 HBV-DNA copies/cell were determined by qPCR and normalized to cell numbers
846 using the single copy gene *PRNP*. Individual animals are indicated relative to the
847 mean value determined in mock treated animals (set to 100 %). A, B, D: Data are
848 given as mean values \pm SD. E: Data points represent individual animals, mean
849 values \pm SD are indicated. ns = not significant, * = $p < 0.05$ (Mann Whitney test).

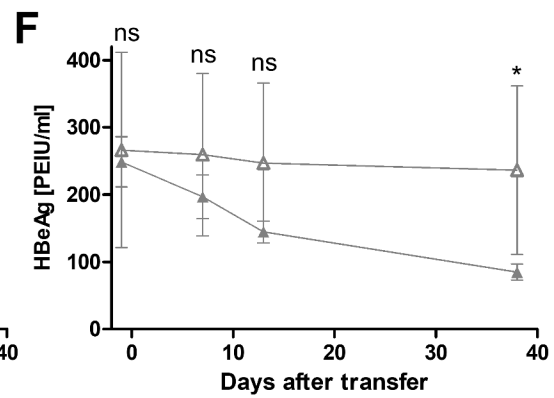
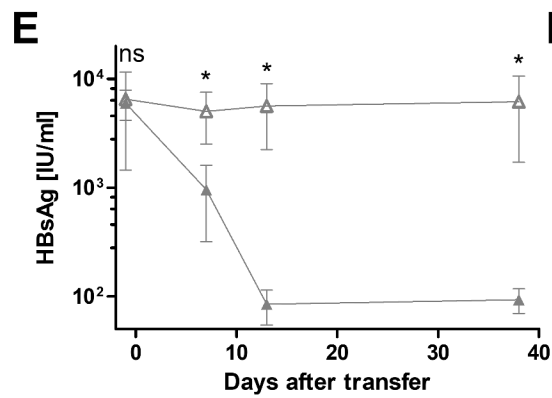
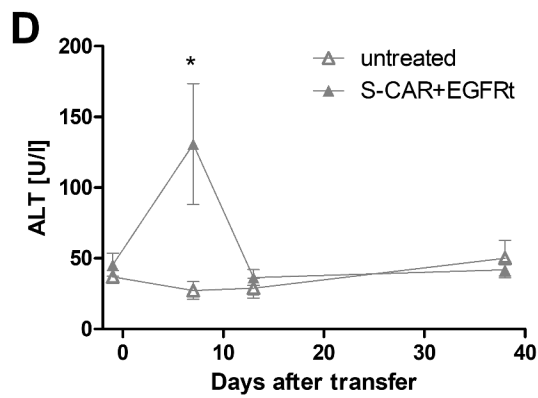
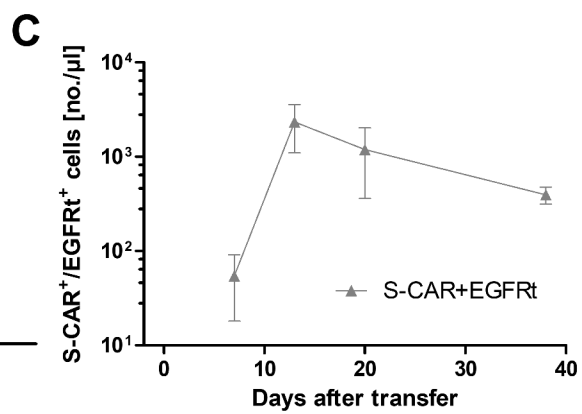
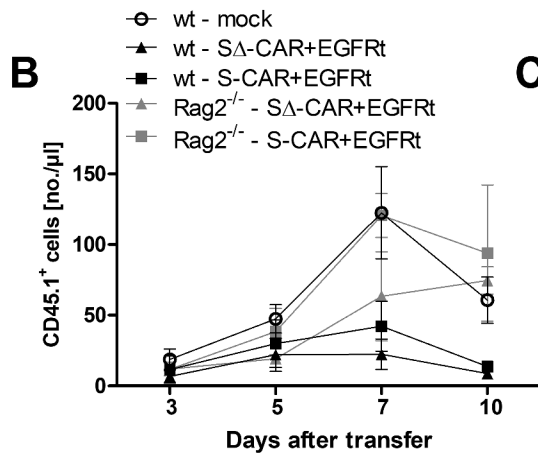
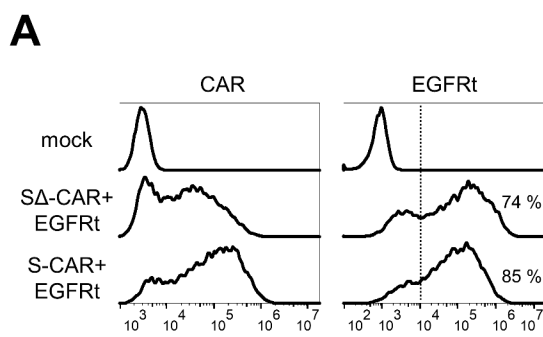
850

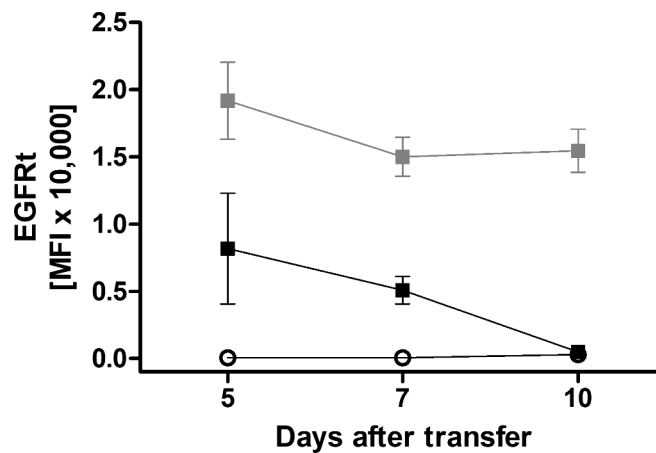
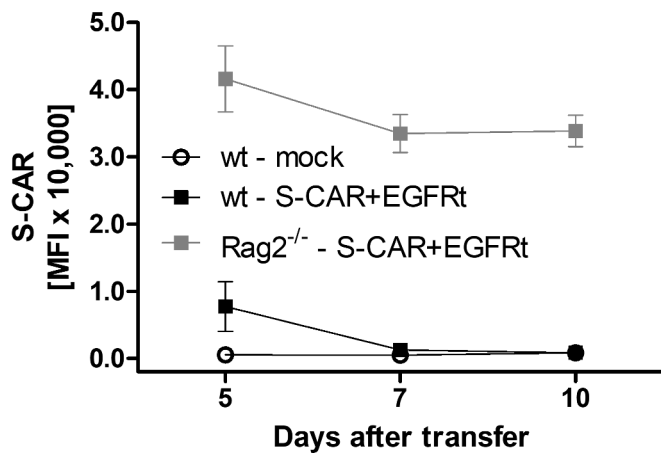
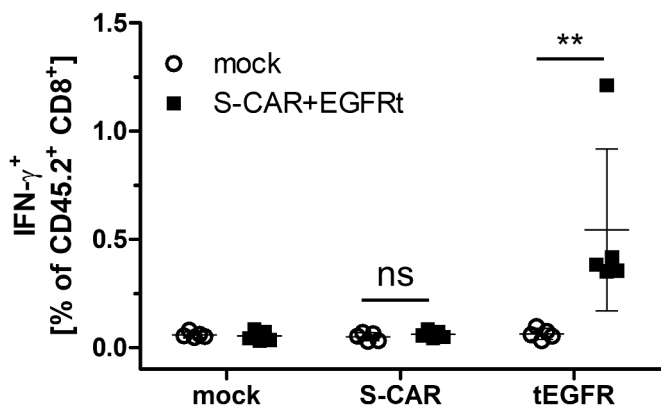
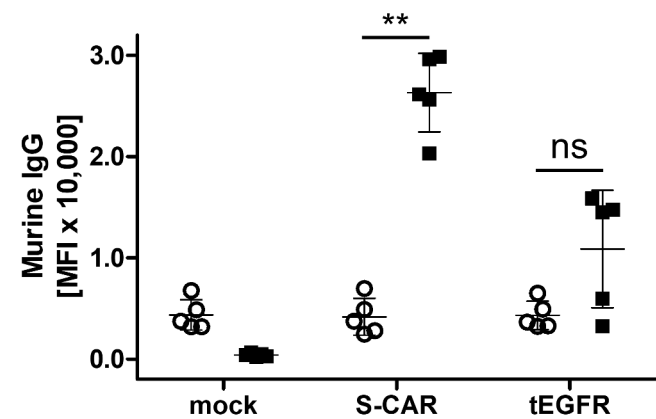
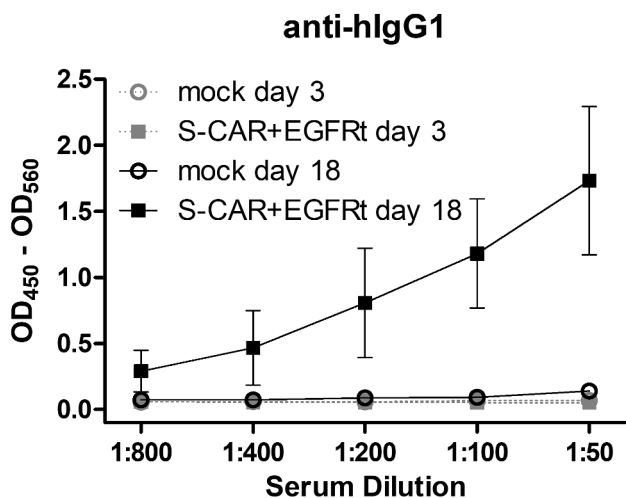
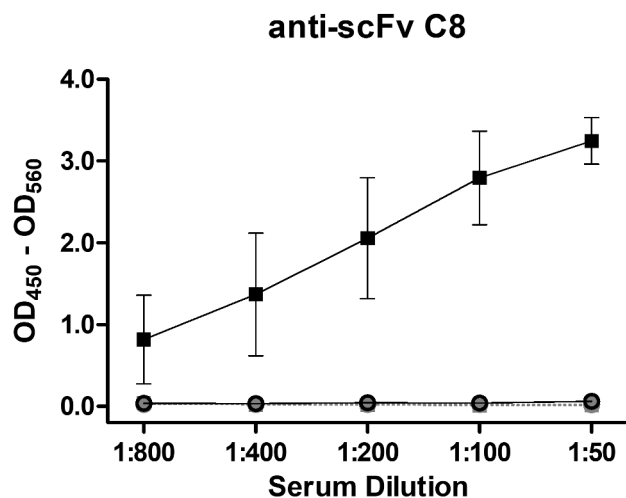
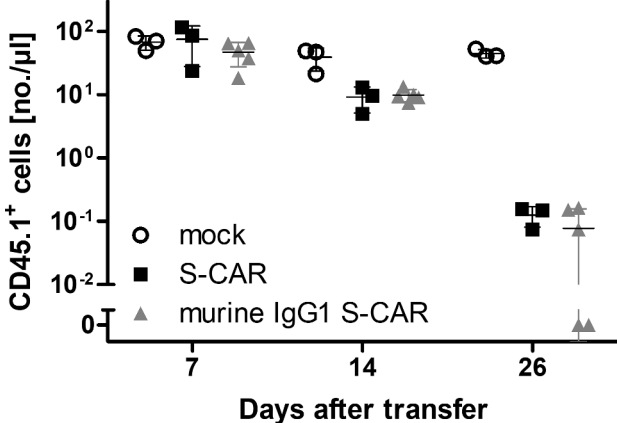
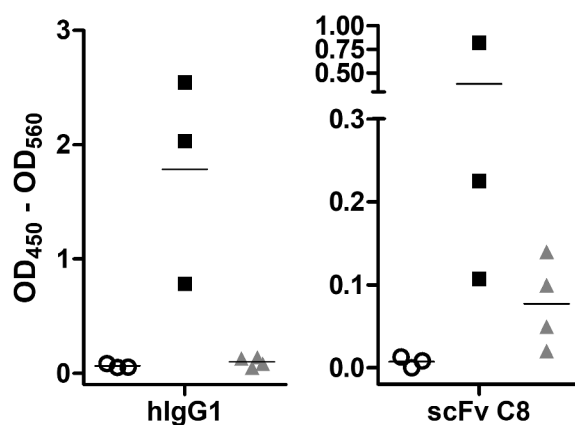
851 **Figure 6: S-CAR T-cell persistence and antiviral effect after tolerization of**
852 **immunocompetent mice.** **A)** Scheme of the experimental procedure. AAV-HBV-
853 infected CD45.2⁺ wildtype mice underwent total body irradiation one day prior to the
854 transfer of 5×10^6 non-functional, CD45.1⁺ S Δ -CAR⁺/EGFR⁺ T cells per animal (n=5
855 per group). 3 months later mice were injected with 3×10^6 functional
856 CD45.1⁺/CD45.2⁺ mock (open circles) or S-CAR⁺ and EGFR⁺ T cells per animal
857 (=day 0). Mice that received S-CAR⁺/EGFR⁺ T cells were either only irradiated (=
858 irradiation, black squares) or were irradiated and received S Δ -CAR⁺/EGFR⁺ T cells
859 (= tolerization, grey triangles). Mice that received mock T cells were not pretreated.
860 Mice were sacrificed 110 days after transfer of functional S-CAR T cells. **B)** Sera

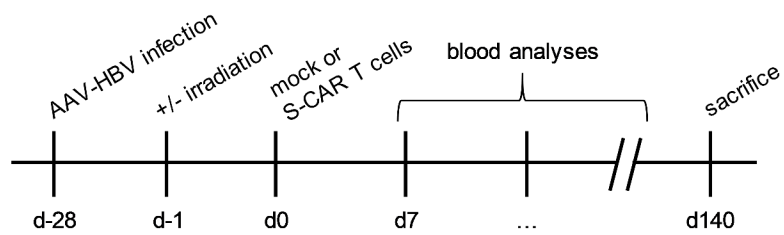
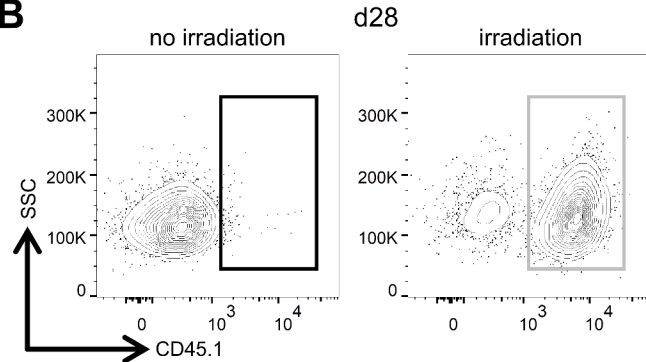
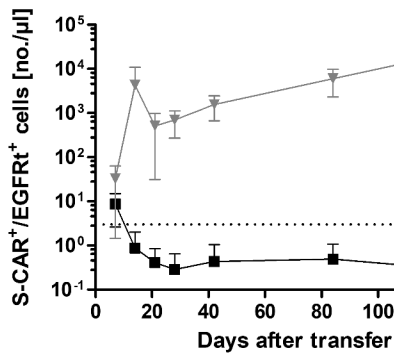
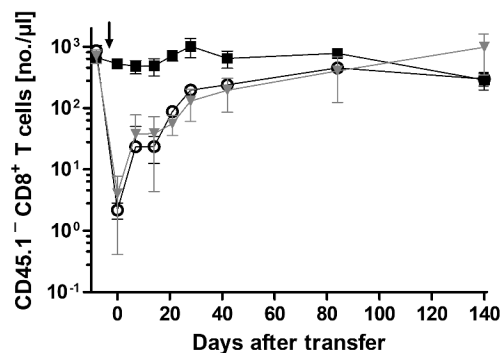
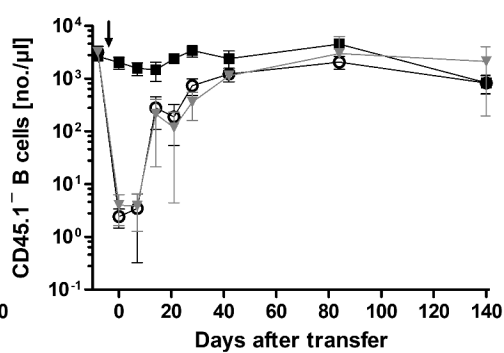
861 from day 27 were analyzed by ELISA for anti-hlgG1 and anti-scFv C8 antibodies. **C)**
862 Splenocytes isolated at the end of the experiment were co-cultured with EGFRt-
863 expressing target cells before ICS. IFN- γ expression of endogenous CD45.1⁻ CD8⁺ T
864 cells upon antigen encounter is shown. **D)** Numbers of CD45.1⁺/CD45.2⁺ S-CAR⁺ or
865 EGFRt⁺ T cells per μ l peripheral blood determined at indicated time points. Dotted
866 line represents the background determined in mock T cell-treated mice. **E)** ALT
867 activity, **F)** HBsAg and **G)** HBeAg levels in serum measured over time. **H)**
868 Intrahepatic AAV- and HBV-DNA copies/cell determined by qPCR normalized to the
869 cellular single copy gene *PRNP*. Values are shown relative to the mean value
870 determined in mock treated mice. D-G: Data are given as mean values \pm SD. B, C, H:
871 Data points represent individual animals, mean values \pm SD are indicated. ns = not
872 significant, * = $p < 0.05$, ** = $p < 0.01$ (Mann Whitney test).

873



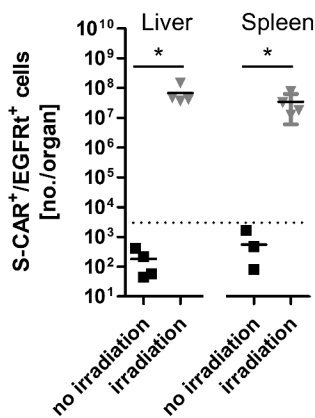
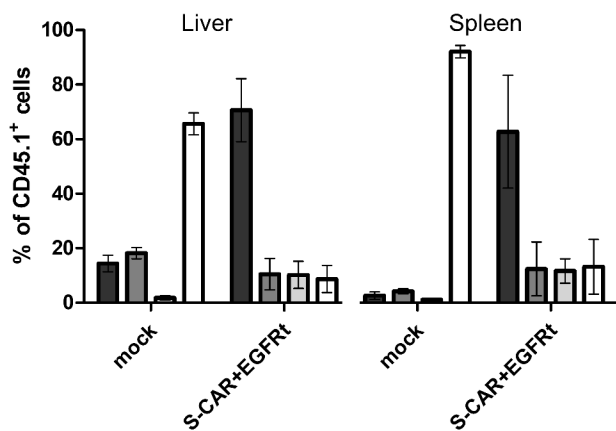
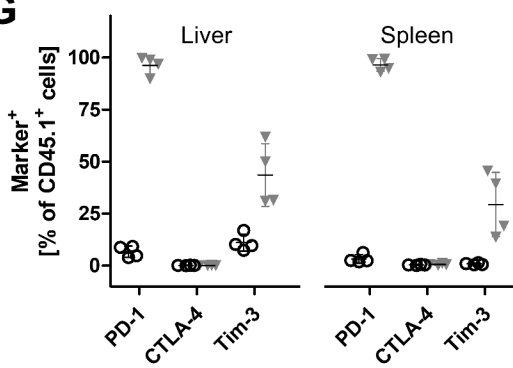
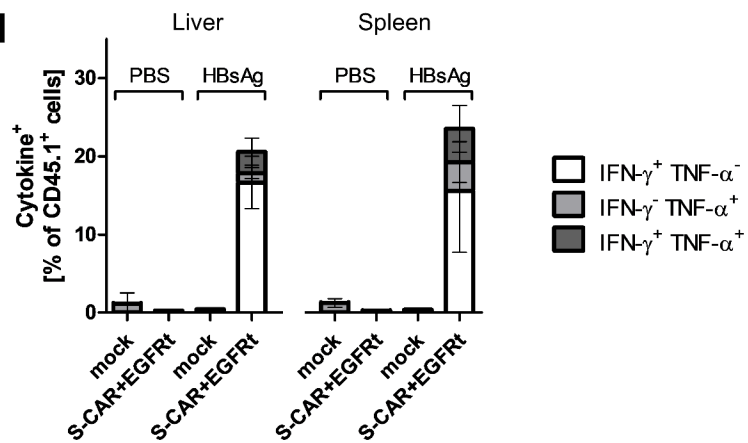
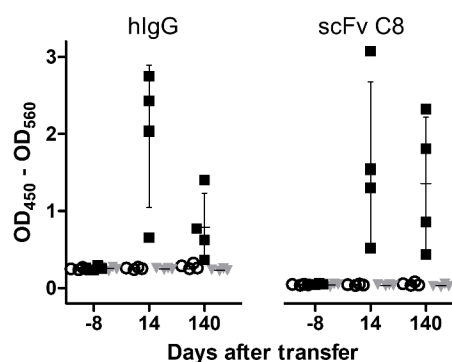


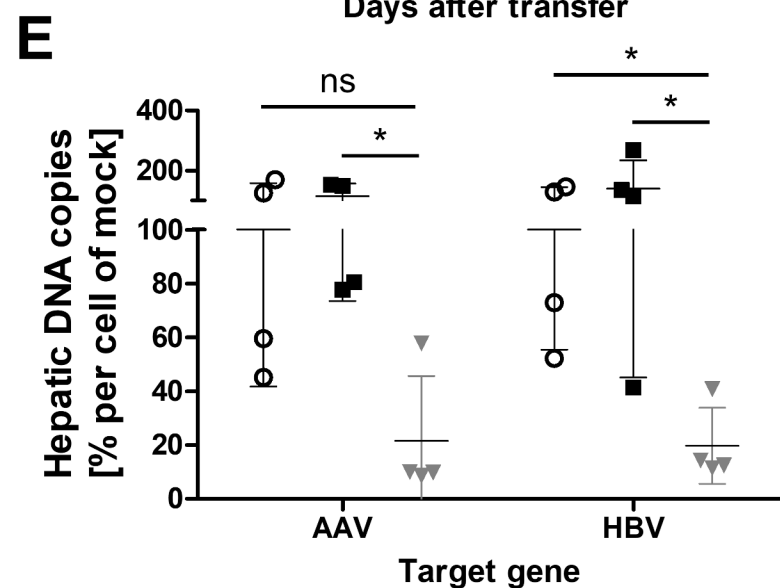
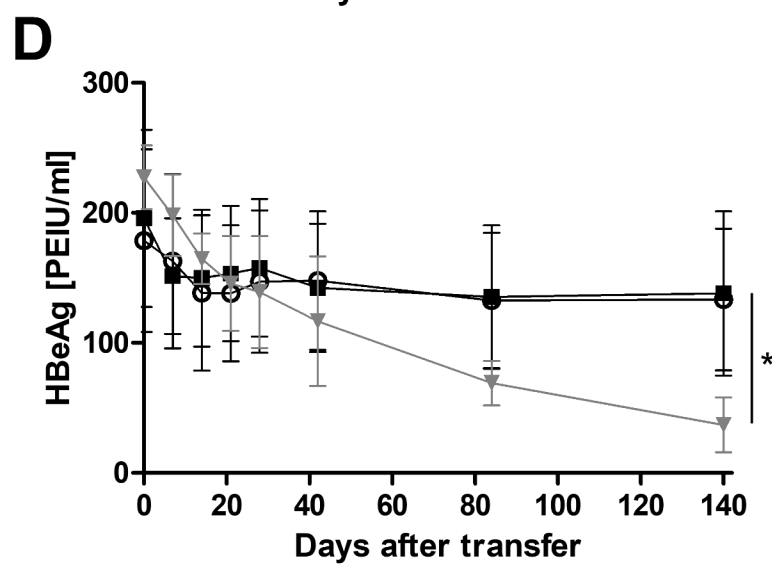
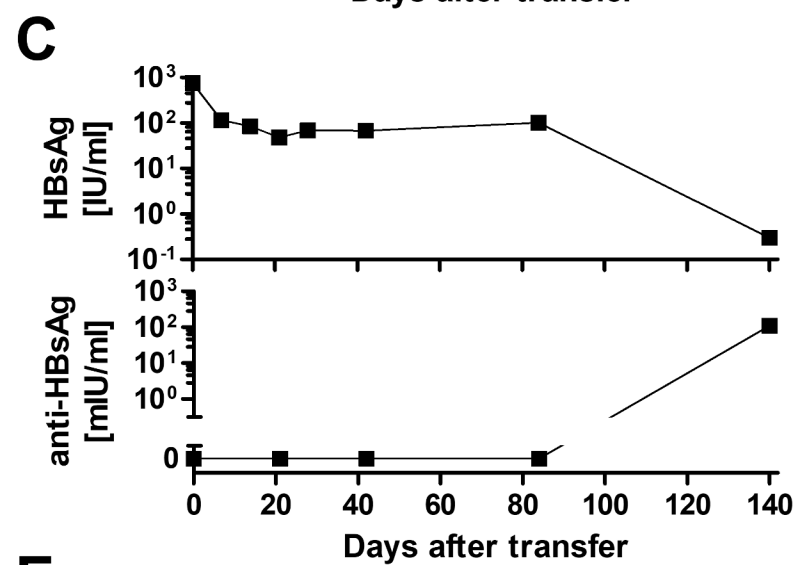
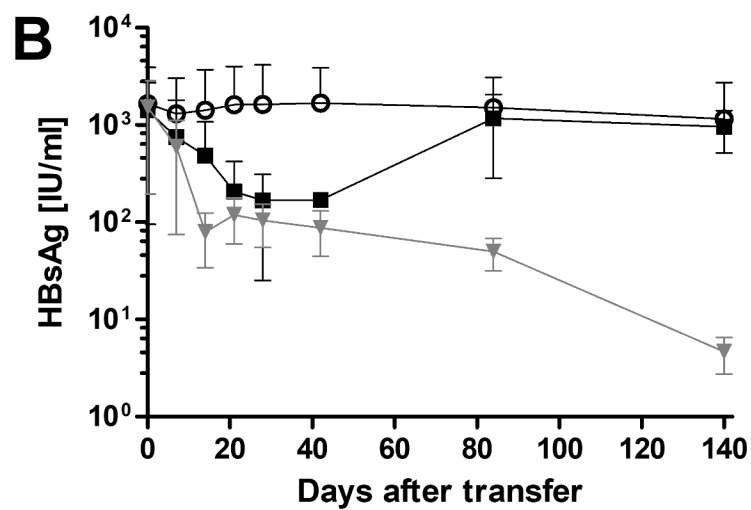
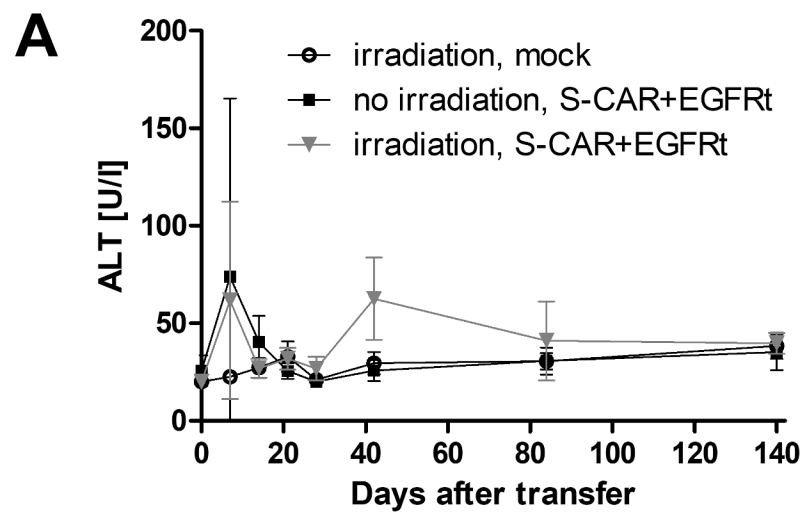
A**B****C****D****E****F****G**

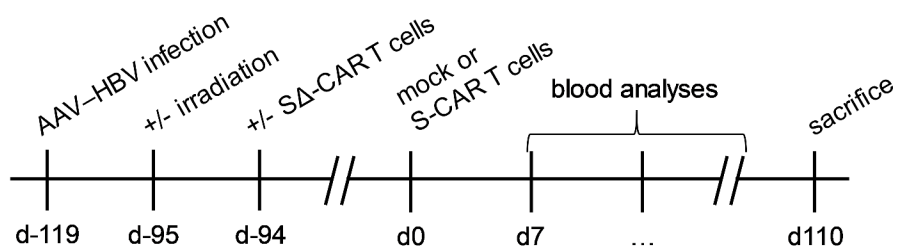
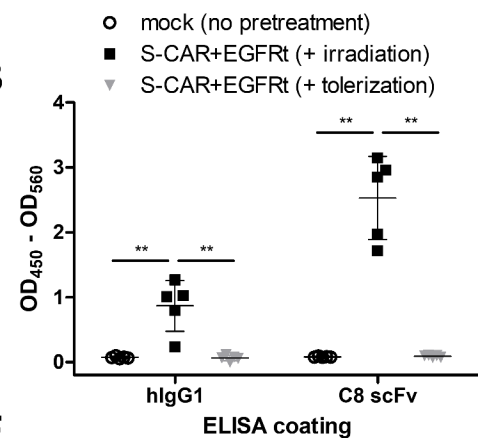
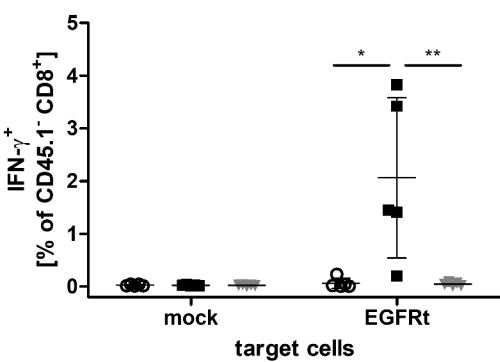
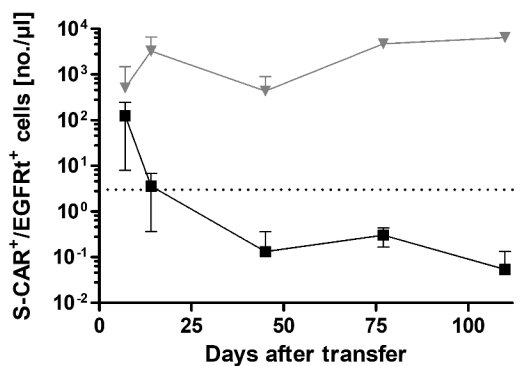
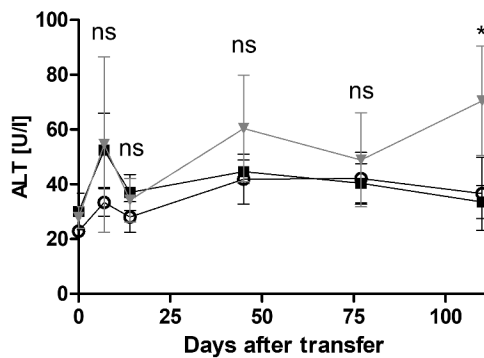
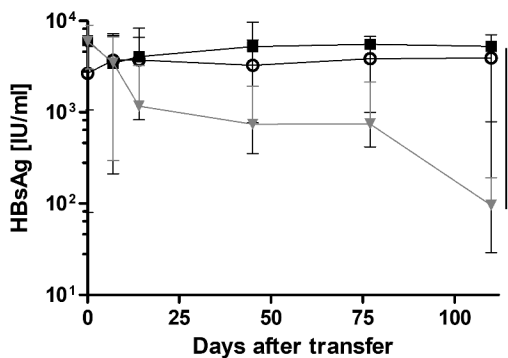
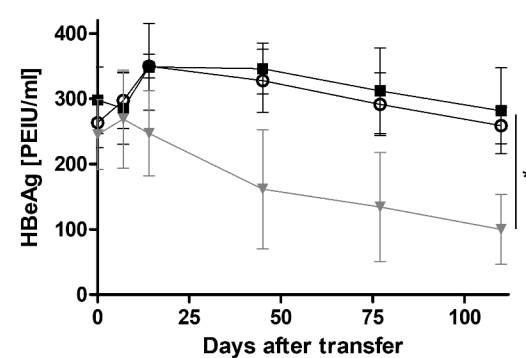
A**B****C****D**

○ irradiation, mock
 ■ no irradiation, S-CAR+EGFRt
 ▽ irradiation, S-CAR+EGFRt

■ Effector
 □ Effector Memory
 ○ Intermediate
 ▽ Naive/Central-Memory

E**F****G****H****I**



A**B****C****D****E****F****G****H**